


Thermal lattice Boltzmann model for liquid-vapor phase changeLei Wang,^{*} Jiangxu Huang, and Kun He*School of Mathematics and Physics, China University of Geosciences, Wuhan 430074, China
and Center for Mathematical Sciences, China University of Geosciences, Wuhan 430074, China* (Received 11 May 2022; revised 23 August 2022; accepted 27 October 2022; published 10 November 2022)

The lattice Boltzmann method is adopted to solve the liquid-vapor phase change problems in this article. By modifying the collision term for the temperature evolution equation, a thermal lattice Boltzmann model is constructed. As compared with previous studies, the most striking feature of the present approach is that it could avoid the calculations of both the Laplacian term of temperature [$\nabla \cdot (\kappa \nabla T)$] and the gradient term of heat capacitance [$\nabla(\rho c_v)$]. In addition, since the present approach adopts a simple linear equilibrium distribution function, it is possible to use the D2Q5 lattice for the two-dimensional cases considered here. Thus, the present model is more efficient than previous models in which the lattice is usually limited to the D2Q9. The proposed model is first validated by the problems of droplet evaporation in open space and droplet evaporation on a heated surface, and the numerical results show good agreement with the analytical results and the finite difference method. Then it is used to model the nucleate boiling problem, and the relationship between detachment bubble diameter and gravitational acceleration obtained with the present approach fits well with previous works.

DOI: [10.1103/PhysRevE.106.055308](https://doi.org/10.1103/PhysRevE.106.055308)**I. INTRODUCTION**

Liquid-vapor phase change processes play a vital role in many industrial applications including nuclear reactor cooling system, power plants, and electronic cooling [1,2]. For decades, many theoretical and experimental studies have been conducted to reveal the fluid flow and heat transfer during liquid-vapor phase change [3–5]. However, due to the various complex phenomena involved in these processes such as interface changes, nonequilibrium effects, or other complex dynamic interaction between the phases, the mechanisms of liquid-vapor phase change heat transfer are still not fully comprehended [6–8]. With recent advances in computer technology, numerical modeling of such problems has attracted great attention due to its ability to provide the details of flow dynamics during liquid-vapor phase change [9–11].

The lattice Boltzmann method (LBM), developed about two decades ago, has gained great success in modeling and simulating of both single-phase and multiphase flows [12–16]. Different from traditional computational fluid dynamics methods based on the macroscopic governing equations, the LBM is actually a mesoscopic numerical approach, and its kinetic characteristics bring some distinctive features to this method, such as the simple algorithm structure, easy boundary treatment, and natural parallelism [17,18]. In recent years the LBM was also adopted by some scholars to simulate liquid-vapor phase change heat transfer such as boiling [19,20] and evaporation [21,22]. These existing LB models usually fall into two main categories: (1) the phase-field method [20,22–24] and (2) the pseudopotential method [19,21,25–28]. For the phase field method [20,22–24], the vapor-liquid

interface is captured by the interface-capturing equation like the Cahn-Hilliard equation, and the phase-change process is established by adding a source term to the interface capturing equation. Also, the energy equation in this approach is used to define the latent heat. To trigger the liquid-vapor phase change, the phase-field method usually assumes an initial vapor profile in the system [20] such that it is not efficient in modeling bubble nucleation in the boiling heat transfer, while this assumption is not required for the pseudopotential method [14]. The key point of the pseudopotential method is that the interaction between different phases is mimicked via an attractive or repulsive force among the neighboring fluid particles [29]. As a consequence, the nonideal gas behavior and phase separation can be realized without using any specific techniques to track or capture interface [13,14,17]. Historically, the pioneering work on simulating liquid-vapor phase change with the pseudopotential method may be attributed to Zhang and Cheng in 2003 [25]. In their work the boiling heat transfer is successfully simulated with the proposed method. Then Hazi and Markus [26] proposed another LB model to simulate the heterogeneous boiling on a horizontal plate. Different from Zhang and Chen's work, the temperature equation in Hazi and Markus's model is derived from the entropy balance equation, and it is coupled with the pseudopotential multiphase LB model through an artificial equation of state (EOS). On the basis of the work of Hazi and Markus, Gong and Cheng [27] developed an improved thermal LB model for liquid-vapor phase change heat transfer by employing the Peng-Robinson EOS. Utilizing this model, they successfully simulated the bubble growth and departure in pool boiling. Subsequently, Li *et al.* [28] pointed out that the replacement of $\nabla \cdot (\kappa \nabla T)/(\rho c_v)$ with $\nabla \cdot [(\kappa/\rho c_v)\nabla T]$ (here κ , ρc_v , and T are the thermal conductivity, heat capacitance, and temperature, respectively) in

^{*}Corresponding author: wangleir1989@126.com

the work of Gong and Cheng is an inappropriate treatment, which will yield considerable errors for the multiphase flows due to the variable density between different phases, and they then proposed another improved thermal LB model for simulation of liquid-vapor phase change. The same authors also constructed a hybrid LB model for liquid-vapor phase change [30], in which the velocity field is solved by using the pseudopotential LB approach, while the temperature field is solved by the finite-difference method. Thereafter, a thermal multiple-relaxation-time (MRT) LB model with a nondiagonal matrix based on the two-dimensional nine-velocity (D2Q9) lattice was developed for liquid-vapor phase change by Zhang *et al.* [31]. Different from the model of Li *et al.* [28], the calculation of the Laplacian term of temperature is avoided in this model, and the latent heat of vaporization is also decoupled with the EOS, and thus it is more flexible in simulating liquid-vapor phase change. However, due to the nondiagonal matrix in this approach relying on the lattice model, it cannot be extended to the three-dimensional case directly. More recently, a three-dimensional thermal LB model was constructed for liquid-vapor phase change by Li *et al.* [32]. Different from previous works, this model is possible to use the D3Q7 lattice due to the convection term in the corresponding LB equation actually treated as a source term, while it still needs to calculate the gradient term of heat capacitance $\nabla(\rho c_v)$.

In this work we propose a thermal LB model for liquid-vapor phase change. By modifying the collision term for the temperature equation, the calculations of the Laplacian term of temperature $[\nabla \cdot (\kappa \nabla T)]$ and the gradient term of heat capacitance $[\nabla(\rho c_v)]$ are both avoided, resulting in the possibility to retain the main advantages of the original LBM. Moreover, due to the present thermal model's being constructed based on a linear equilibrium distribution, it is possible to use a more simple D2Q5 lattice, and also a D3Q7 lattice when it is extended to 3D space. The rest of the paper is organized as follows. In Sec. II a pseudopotential model is briefly introduced. Then a thermal LB model is proposed in Sec. III. Numerical validation of the proposed model is presented in Sec. IV. Finally, a brief summary is concluded in Sec. V.

II. PSEUDOPOTENTIAL LATTICE BOLTZMANN MODEL

The pseudopotential multiphase model, originally proposed by Shan and Chen [29], is a particularly popular method in the LB community for its simplicity and intuitive connection to classical nonideal gas EOS [33]. To achieve the thermodynamic consistency, various improved pseudopotential models have been proposed in the past two decades [34–36]. In this work, an improved D2Q9 multiple-relaxation-time (MRT) pseudopotential model developed by Li *et al.* [34] is considered, and the evolution equation of the density distribution f_i in this model is written as

$$\begin{aligned} & f_i(\mathbf{x} + \mathbf{c}_i \Delta t, t + \Delta t) - f_i(\mathbf{x}, t) \\ &= -(\mathbf{M}^{-1} \mathbf{S} \mathbf{M})_{ij} [f_j(\mathbf{x}, t) - f_j^{(eq)}(\mathbf{x}, t)] + \Delta t F'_i(\mathbf{x}, t), \end{aligned} \quad (1)$$

in which \mathbf{c}_i is the discrete velocity at position \mathbf{x} and time t . For the D2Q9 model considered here, the discrete velocities are defined as [17]

$$\mathbf{c}_i = \begin{cases} (0, 0), & i = 0, \\ (\cos[(i-1)\pi/2], \sin[(i-1)\pi/2])c, & i = 1-4, \\ (\cos[(2i-9)\pi/4], \sin[(2i-9)\pi/4])\sqrt{2}c, & i = 5-8, \end{cases} \quad (2)$$

where $c = \Delta x / \Delta t$ is the lattice speed with Δx and Δt denoting the lattice spacing and time step (both are set to 1 in the present work). $f_i^{(eq)}(\mathbf{x}, t)$ is the equilibrium distribution given by [37]

$$f_i^{(eq)}(\mathbf{x}, t) = \omega_i \rho \left[1 + \frac{\mathbf{c}_i \cdot \mathbf{u}}{c_s^2} + \frac{(\mathbf{c}_i \cdot \mathbf{u})^2}{2c_s^4} - \frac{|\mathbf{u}|^2}{2c_s^2} \right], \quad (3)$$

where ω_i is the weight coefficient given by $\omega_0 = 4/9$, $\omega_{1-4} = 1/9$, $\omega_{5-8} = 1/36$, $\mathbf{u} = (u_x, u_y)$ is the velocity, and $c_s = c/\sqrt{3}$ is the sound speed. \mathbf{M} is the transformation matrix given by [38]

$$\begin{bmatrix} 1 & 1 & 1 & 1 & 1 & 1 & 1 & 1 & 1 \\ -4 & -1 & -1 & -1 & -1 & 2 & 2 & 2 & 2 \\ 4 & -2 & -2 & -2 & 1 & 1 & 1 & 1 & 1 \\ 0 & 1 & 0 & -1 & 0 & 1 & -1 & -1 & 1 \\ 0 & -2 & 0 & 2 & 0 & 1 & -1 & -1 & 1 \\ 0 & 0 & 1 & 0 & -1 & 1 & 1 & -1 & -1 \\ 0 & 0 & -2 & 0 & 2 & 1 & 1 & -1 & -1 \\ 0 & 1 & -1 & 1 & -1 & 0 & 0 & 0 & 0 \\ 0 & 0 & 0 & 0 & 0 & 1 & -1 & 1 & -1 \end{bmatrix}. \quad (4)$$

Note that when Eq. (1) is multiplied by the transformation matrix \mathbf{M} , the original collision step implemented in velocity space will turn to execute in the momentum space,

$$\begin{aligned} \mathbf{m}^*(\mathbf{x}, t) &= \mathbf{m}(\mathbf{x}, t) - \mathbf{S}[\mathbf{m}(\mathbf{x}, t) - \mathbf{m}^{eq}(\mathbf{x}, t)] \\ &+ \Delta t \left(\mathbf{I} - \frac{\mathbf{S}}{2} \right) \mathbf{F}(\mathbf{x}, t), \end{aligned} \quad (5)$$

while the streaming step is still implemented in the velocity space,

$$f_i(\mathbf{x} + \mathbf{c}_i \Delta t, t + \Delta t) = f_i^*(\mathbf{x}, t). \quad (6)$$

Here $\mathbf{m}(\mathbf{x}, t) = \mathbf{M} \mathbf{f}$ is the rescaled moment with $\mathbf{f}(\mathbf{x}, t) = [f_0(\mathbf{x}, t), \dots, f_8(\mathbf{x}, t)]^T$, and $f_i^*(\mathbf{x}, t) = \mathbf{M}^{-1} \mathbf{m}^*(\mathbf{x}, t)$ is the postcollision distribution function, \mathbf{I} is the unit matrix, and $\mathbf{S} = \text{diag}(s_0, s_e, s_\varepsilon, s_j, s_q, s_j, s_q, s_p, s_p)$ is the diagonal relaxation matrix. $\mathbf{m}^{eq}(\mathbf{x}, t)$ is the equilibrium function in the moment space given by

$$\begin{aligned} \mathbf{m}^{eq}(\mathbf{x}, t) &= \rho [1, -2 + 3|\mathbf{u}|^2, 1 - 3|\mathbf{u}|^2, u_x, -u_x, u_y, \\ &- u_y, u_x^2 - u_y^2, u_x u_y]^T. \end{aligned} \quad (7)$$

In addition, $\mathbf{F}(\mathbf{x}, t)$ is the forcing term in the moment space satisfying $(\mathbf{I} - 0.5\mathbf{S})\mathbf{F}(\mathbf{x}, t) = \mathbf{M} \mathbf{F}'$. Following the work of Li

et al. [34], it can be written as

$$\mathbf{F} = \begin{bmatrix} 0 \\ 6\mathbf{u} \cdot \mathbf{F}_n + \frac{\sigma |\mathbf{F}_m|^2}{\psi^2 \Delta t (s_e^{-1} - 0.5)} \\ -6\mathbf{u} \cdot \mathbf{F}_n - \frac{\sigma |\mathbf{F}_m|^2}{\psi^2 \Delta t (s_e^{-1} - 0.5)} \\ F_{n,x} \\ -F_{n,x} \\ F_{n,y} \\ -F_{n,y} \\ 2(u_x F_{n,x} - u_y F_{n,y}) \\ u_x F_{n,y} + u_y F_{n,x} \end{bmatrix}, \quad (8)$$

where σ is a tunable parameter used to achieve thermodynamic consistency and $\mathbf{F}_n = (F_{n,x}, F_{n,y})$ is the total force, and it is defined as $\mathbf{F}_n = \mathbf{F}_m + \mathbf{F}_b$, with \mathbf{F}_b and \mathbf{F}_m representing the external force and the intermolecular interaction force, respectively. For the D2Q9 lattice considered here, the interaction force is given by [39]

$$\mathbf{F}_m = -G\psi(\mathbf{x}) \sum_{i=1}^8 \varpi(|\mathbf{c}_i \Delta t|^2) \psi(\mathbf{x} + \mathbf{c}_i \Delta t) \mathbf{c}_i \Delta t, \quad (9)$$

where $\varpi(|\mathbf{c}_i \Delta t|^2)$ are the weights, which are given as $\varpi(\Delta x^2) = 1/3$, $\varpi(2\Delta x^2) = 1/12$, G is a parameter that controls the strength of the interparticle force, whose value is usually set to be -1 in many simulations, and $\psi(\mathbf{x})$ is the mean-field potential, which is calculated from $\psi(\mathbf{x}) = \sqrt{2(p_{EOS} - \rho c_s^2)/(G\Delta x^2)}$ with p_{EOS} being the nonideal EOS [33]. In the present work, the Peng-Robinson EOS is used [13], which is given as

$$p_{EOS} = \frac{\rho RT}{1 - b\rho} - \frac{a\varphi(T)\rho^2}{1 + 2b\rho - b^2\rho^2}, \quad (10)$$

where R is the gas constant, $a = 0.45724R^2 T_c^2 / p_c$, and $b = 0.0778RT_c / p_c$, with T_c and p_c representing the critical temperature and the critical pressure, respectively. $\varphi(T) = [1 + (0.37464 + 1.54226\bar{\omega} - 0.26992\bar{\omega}^2)(1 - \sqrt{T/T_c})]^2$, in which $\bar{\omega} = 0.344$ is the acentric factor and T is the temperature, and it is calculated from the energy equation in the real simulations. For the other parameters, we choose $a = 3/49$, $b = 2/21$, and $R = 1$, which have been widely used in previous works. Finally, the macroscopic density ρ and velocity \mathbf{u} in the pseudopotential model are calculated by

$$\rho = \sum_{i=0}^8 f_i, \quad \rho \mathbf{u} = \sum_{i=0}^8 \mathbf{c}_i f_i + \frac{\Delta t}{2} \mathbf{F}_n. \quad (11)$$

III. NUMERICAL FORMULATIONS

A. Reexamination of previous lattice Boltzmann models

Before proceeding further, the governing equation for liquid-vapor phase change is first revisited. According to the work of Anderson *et al.* [40], by neglecting the effect of viscous heat dissipation, the energy equation for liquid-vapor phase change can be expressed as (also called the local balance law for entropy)

$$\rho T \frac{Ds}{Dt} = \nabla \cdot (\lambda \nabla T), \quad (12)$$

where $D(\cdot)/Dt = \partial_t(\cdot) + \mathbf{u} \cdot \nabla(\cdot)$ is the material derivative, s is the entropy, and λ is the thermal conductivity. To simplify the above equation, the following thermodynamic relation is considered [41]:

$$ds = \frac{c_v}{T} dT + \left(\frac{\partial p_{EOS}}{\partial T} \right)_\rho d\left(\frac{1}{\rho}\right) \quad (13)$$

in which c_v is the specific heat at constant volume. According to Eq. (13), and note that the continuity equation $D\rho/Dt = -\rho \nabla \cdot \mathbf{u}$, the temperature equation for liquid-vapor phase change can be written as

$$\rho c_v \frac{\partial T}{\partial t} + \rho c_v \mathbf{u} \cdot \nabla T = \nabla \cdot (\lambda \nabla T) - T \left(\frac{\partial p_{EOS}}{\partial T} \right)_\rho \nabla \cdot \mathbf{u}. \quad (14)$$

In order to solve the above equation within the framework of LBM, various models have been proposed in previous works [27,28,31,32]; however, the evolution equations that appeared in these existing works are rather heuristic. In fact, to match the corresponding thermal LB models, these models are almost constructed based on the following variant temperature equation [27,28,31,32]:

$$\frac{\partial T}{\partial t} + \nabla \cdot (\mathbf{u}T) = \nabla \cdot (\eta \nabla T) + R, \quad (15)$$

where η is the thermal diffusivity or an artificial parameter depending on the expression of the source term of R . Since Eq. (15) is a standard convection-diffusion equation with a source term, many universal models can be adopted for solving this equation in the LB community [42–44]. Following this idea, Gong and Cheng [27] proposed an LB model for liquid-vapor phase change where

$$\eta = \frac{\lambda}{\rho c_v}, \quad R = T \left[1 - \frac{1}{\rho c_v} \left(\frac{\partial p_{EOS}}{\partial T} \right)_\rho \right] \nabla \cdot \mathbf{u}. \quad (16)$$

Comparing Eq. (16) with Eq. (14), one can find that the term of $\nabla \cdot (\lambda \nabla T) / (\rho c_v)$ is replaced by $\nabla \cdot \{[\lambda / (\rho c_v)] \nabla T\}$ in the Gong and Cheng model. Although this treatment is acceptable for the single-phase flow in the incompressible limit, it is not correct for the multiphase flows, especially for the liquid-vapor interface, where the density varies significantly. In this setting, Li *et al.* [28] proposed an improved LBM, and in their model,

$$\begin{aligned} \eta &= k, \\ R &= \frac{1}{\rho c_v} \nabla \cdot (\lambda \nabla T) - \nabla \cdot (k \nabla T) \\ &\quad + T \left[1 - \frac{1}{\rho c_v} \left(\frac{\partial p_{EOS}}{\partial T} \right)_\rho \right] \nabla \cdot \mathbf{u}, \end{aligned} \quad (17)$$

where k is an artificial parameter. For this model, due to the source term R being related to the Laplacian or gradient term of temperature, one must calculate it with the help of a finite-difference scheme, making it unable to hold the advantages of the LBM very well. In addition, Zhang *et al.* [31] also proposed another improved thermal LBM for liquid-vapor

phase change where

$$\eta = \frac{\lambda}{\rho c_v},$$

$$R = \frac{\lambda \nabla T \cdot \nabla(\rho c_v)}{(\rho c_v)^2} + \left(T - \frac{\rho H}{c_v} - \frac{p_{EOS}}{\rho c_v} \right) \nabla \cdot \mathbf{u}, \quad (18)$$

in which H is a parameter related to the latent heat of vaporization. In contrast to the model of Li *et al.*, this model is not necessary to calculate the Laplacian of temperature, and the latent heat is decoupled with the EOS. However, it still needs to calculate the gradient term of $\nabla(\rho c_v)$ with the finite-difference scheme, which will bring some numerical errors into the system. This phenomenon may be more remarkable around the liquid-vapor interface. On the other hand, since the calculation of temperature in the model of Zhang *et al.* is related to the source term R , causing the corresponding expression to be implicit, an iteration procedure is needed theoretically. Apart from the above models, Li *et al.* [32] recently also proposed a 3D thermal LBM for phase change heat transfer in which

$$\eta = \frac{\lambda}{\rho c_v},$$

$$R = \frac{\lambda \nabla T \cdot \nabla(\rho c_v)}{(\rho c_v)^2} - \mathbf{u} \cdot \nabla T - \frac{T}{\rho c_v} \left(\frac{\partial p_{EOS}}{\partial T} \right)_\rho \nabla \cdot \mathbf{u} + \nabla \cdot (\mathbf{u}T). \quad (19)$$

Substituting Eq. (19) into Eq. (15), one can find that the convection term in the temperature equation (14) is actually treated as a source term in this model; however, the calculation of $\nabla(\rho c_v)$ still exists.

B. Thermal lattice Boltzmann model

In this section we propose a thermal LB model for liquid-vapor phase change. To this end the temperature equation is changed to

$$\rho c_v \frac{\partial T}{\partial t} = \nabla \cdot (\lambda \nabla T) - \left[\rho c_v \mathbf{u} \cdot \nabla T + T \left(\frac{\partial p_{EOS}}{\partial T} \right)_\rho \nabla \cdot \mathbf{u} \right]. \quad (20)$$

Apparently, the above equation can be viewed as a pure diffusion equation $\rho c_v \partial_t T = \nabla \cdot (\lambda \nabla T) + Q$ with a corresponding source term $Q = -[\rho c_v \mathbf{u} \cdot \nabla T + T(\partial p_{EOS}/\partial T)_\rho \nabla \cdot \mathbf{u}]$. Although it is not difficult to develop an LBM for solving the pure diffusion equation [45,46], how to incorporate ρc_v in front of $\partial T/\partial t$ into the temperature evolution equation is a problem that must be addressed. Inspired by the work of Cartalade *et al.* [47], a thermal LB model is proposed for simulating liquid-vapor phase change. To have a better understanding of the proposed LBM, we first present the model by using the simplest Bhatnagar-Gross-Krook (BGK) operator, and then extend it to the multiple-relaxation-time (MRT) model, which is a generalized model and has distinct advantages over the BGK model in terms of stability and accuracy.

1. BGK model for liquid-vapor phase change

The lattice BGK equation for the temperature distribution function g_i is expressed as

$$\rho c_v g_i(\mathbf{x} + \mathbf{c}_i \Delta t, t + \Delta t) - g_i(\mathbf{x}, t)$$

$$= (\rho c_v - 1) g_i(\mathbf{x} + \mathbf{c}_i \Delta t, t) - \frac{1}{\tau_g} [g_i(\mathbf{x}, t) - g_i^{(eq)}(\mathbf{x}, t)]$$

$$+ \Delta t G_i + \Delta t S_i, \quad (21)$$

where τ_g is the relaxation time, $g_i^{(eq)}$ is the local equilibrium distribution function defined as

$$g_i^{(eq)} = \hat{w}_i T, \quad (22)$$

G_i is the source term given by

$$G_i = -\hat{w}_i [\rho c_v \mathbf{u} \cdot \nabla T + T(\partial_T p_{EOS})_\rho \nabla \cdot \mathbf{u}], \quad (23)$$

and the correction term S_i is chosen as

$$S_i = \hat{w}_i \rho c_v \frac{\Delta t}{2} \partial_i^2 T. \quad (24)$$

The temperature T is calculated from

$$T = \sum_i g_i. \quad (25)$$

Since the equilibrium distribution function is a linear form, it is possible to use a simpler D2Q5 lattice model, in which the discrete velocity set is expressed as

$$\mathbf{c}_i = \begin{cases} (0, 0), & i = 0 \\ (\cos[(i-1)\pi/2], \sin[(i-1)\pi/2])c, & i = 1-4 \end{cases} \quad (26)$$

and the corresponding weight coefficient in such a case can be defined as $\hat{w}_{i=0} = 1 - \hat{w}$, $\hat{w}_{i=1-4} = \hat{w}/4$ [\hat{w} is a parameter satisfying $\hat{w} \in (0, 1)$] with the sound speed given by $\hat{c}_s^2 = \hat{w}/2$ [48].

To recover the macroscopic temperature equation from the lattice BGK equation, in what follows we will perform a multiscale analysis of the present model. To this end, the distribution function g_i and the time and space derivatives are first expanded as [18]

$$g_i = g_i^{(0)} + \epsilon g_i^{(1)} + \epsilon^2 g_i^{(2)}, \quad \partial_t = \epsilon \partial_{t_1} + \epsilon^2 \partial_{t_2}, \quad \nabla = \epsilon \nabla_1, \quad (27)$$

where t_1 is the fast convective scale, t_2 is the slow diffusive scale, and ϵ is a small parameter which is proportional to the Knudsen number in the classical kinetic theory for fluid flows.

By Taylor expansion the lattice BGK equation yields

$$\rho c_v \left(g_i + \Delta t D_i g_i + \frac{\Delta t^2}{2} D_i^2 g_i \right)$$

$$- g_i + (1 - \rho c_v) \left(g_i + \Delta t d_i g_i + \frac{\Delta t^2}{2} d_i^2 g_i \right)$$

$$= -\frac{1}{\tau_g} (g_i - g_i^{(eq)}) + \Delta t G_i + \Delta t S_i, \quad (28)$$

where $D_i = \partial_t + d_i$ with $d_i = \mathbf{c}_i \cdot \nabla$. Then substituting Eq. (27) into Eq. (28), and equating the coefficients of each

order of ϵ , we have

$$O(\epsilon^0): g_i^{(0)} = g_i^{(eq)}, \quad (29)$$

$$O(\epsilon^1): \rho c_v \partial_{t_1} g_i^{(0)} + d_{1i} g_i^{(0)} = -\frac{1}{\tau_g \Delta t} g_i^{(1)} + \hat{w}_i Q^{(1)}, \quad (30)$$

$$\begin{aligned} O(\epsilon^2): & \rho c_v D_{1i} g_i^{(1)} + \rho c_v \partial_{t_2} g_i^{(0)} + \rho c_v \frac{\Delta t}{2} D_{1i}^2 g_i^{(0)} \\ & + (1 - \rho c_v) d_{1i} g_i^{(1)} + (1 - \rho c_v) \frac{\Delta t}{2} d_{1i}^2 g_i^{(0)} \\ & = -\frac{1}{\tau_g \Delta t} g_i^{(2)} + \hat{w}_i \rho c_v \frac{\Delta t}{2} (\partial_{t_1})^2 T, \end{aligned} \quad (31)$$

where $D_{1i} = \partial_{t_1} + d_{1i} = \partial_{t_1} + \mathbf{c}_i \cdot \nabla_1$. If we expand D_{1i} and D_{1i}^2 in Eq. (31), then the corresponding equation can be rewritten as

$$\begin{aligned} & \rho c_v \partial_{t_1} g_i^{(1)} + d_{1i} g_i^{(1)} + \rho c_v \partial_{t_2} g_i^{(0)} + \rho c_v \frac{\Delta t}{2} \partial_{t_1}^2 g_i^{(0)} \\ & + \rho c_v \frac{\Delta t}{2} (2\partial_{t_1} d_{1i}) g_i^{(0)} + \frac{\Delta t}{2} d_{1i}^2 g_i^{(0)} \\ & = -\frac{1}{\tau_g \Delta t} g_i^{(2)} + \hat{w}_i \rho c_v \frac{\Delta t}{2} (\partial_{t_1})^2 T. \end{aligned} \quad (32)$$

From Eqs. (22)–(24) and Eq. (29), one can obtain that

$$\begin{aligned} \sum_i g_i^{(0)} &= T, \quad \sum_i \mathbf{c}_i g_i^{(0)} = 0, \quad \sum_i \mathbf{c}_i \mathbf{c}_i g_i^{(0)} = \hat{c}_s^2 T \mathbf{I}, \\ \sum_i S_i &= \rho c_v \frac{\Delta t}{2} \partial_t^2 T, \quad \sum_i \mathbf{c}_i S_i = 0, \quad \sum_i G_i = Q, \\ \sum_i \mathbf{c}_i G_i &= 0. \end{aligned} \quad (33)$$

Summing Eqs. (30) and (32) over i with the help of Eq. (33), and noting that $d_{1i}^2 = \nabla_1 \nabla_1 : \mathbf{I}$, we obtain

$$\rho c_v \partial_{t_1} T = Q^{(1)}, \quad (34)$$

$$\nabla_1 \cdot \sum_i \mathbf{c}_i g_i^{(1)} + \rho c_v \partial_{t_2} T + \frac{\Delta t}{2} \nabla_1 \nabla_1 : \hat{c}_s^2 T \mathbf{I} = 0. \quad (35)$$

In order to evaluate $\sum_i \mathbf{c}_i g_i^{(1)}$ in Eq. (35), we multiply Eq. (30) by \mathbf{c}_i and taking summation over i ,

$$\begin{aligned} -\frac{1}{\tau_g \Delta t} \sum_i \mathbf{c}_i g_i^{(1)} &= \rho c_v \partial_{t_1} \sum_i \mathbf{c}_i g_i^{(0)} + \nabla_1 \cdot \sum_i \mathbf{c}_i \mathbf{c}_i g_i^{(0)} \\ &\quad - \sum_i \hat{w}_i \mathbf{c}_i Q^{(1)} \\ &= \hat{c}_s^2 \nabla_1 T. \end{aligned} \quad (36)$$

Substituting Eq. (36) into Eq. (35) yields

$$\rho c_v \partial_{t_2} T = \nabla_1 \cdot \left(\tau_g - \frac{1}{2} \right) \Delta t \hat{c}_s^2 \nabla_1 T. \quad (37)$$

Based on Eqs. (34) and (37), we obtain

$$\rho c_v \partial_t T = \nabla \cdot \left(\tau_g - \frac{1}{2} \right) \hat{c}_s^2 \Delta t \nabla T + Q. \quad (38)$$

Comparing Eq. (38) with Eq. (30), the dimensionless relaxation time τ_g is determined by $\lambda = \hat{c}_s^2 (\tau_g - \frac{1}{2}) \Delta t$.

Through the above multiscale analysis, it is clear that the temperature equation is recovered without any deviation terms. In addition, although a temperature space derivative appears in the discrete source term of G_i , it can be computed locally using Eq. (36) with $\epsilon g_i^{(1)} \approx g_i - g_i^{(eq)}$. More importantly, the calculations of $\nabla \cdot (\kappa \nabla T)$ or $\nabla(\rho c_v)$ do not appear in the present scheme, such that the formulation of the present LBM is more concise in contrast to previous models, and therefore, it holds the advantages of the original LBM very well.

2. MRT model for liquid-vapor phase change

We now turn to extend the above BGK model to the MRT version, and the evolution equation with a MRT collision operator $\hat{\mathbf{M}}$ can be expressed as

$$\begin{aligned} & \rho c_v g_i(\mathbf{x} + \mathbf{c}_i \Delta t, t + \Delta t) \\ & = g_i(\mathbf{x}, t) + (\rho c_v - 1) g_i(\mathbf{x} + \mathbf{c}_i \Delta t, t) \\ & \quad - (\hat{\mathbf{M}}^{-1} \Lambda \hat{\mathbf{M}})_{ij} [g_j(\mathbf{x}, t) - g_j^{(eq)}(\mathbf{x}, t)] + \Delta t G_i + \Delta t S_i, \end{aligned} \quad (39)$$

where Λ is a nonnegative diagonal relaxation matrix given by $\Lambda = (\zeta_0, \zeta_1, \dots, \zeta_4)$ with $\zeta_i \in (0, 1)$. Unlike most previous MRT models based on the orthogonal transformation matrix, the present MRT scheme is constructed using a nonorthogonal one, which is simpler and more efficient because it contains more zero elements than the orthogonal transformation matrix [48]. For the D2Q5 lattice considered here, the nonorthogonal transformation matrix $\hat{\mathbf{M}}$ is defined as [49,50]

$$\hat{\mathbf{M}} = \begin{bmatrix} 1 & 1 & 1 & 1 & 1 \\ 0 & 1 & 0 & -1 & 0 \\ 0 & 0 & 1 & 0 & -1 \\ 0 & 1 & 1 & 1 & 1 \\ 0 & 1 & -1 & 1 & -1 \end{bmatrix}. \quad (40)$$

The aforementioned multiscale analysis is adopted again to show that the temperature equation can be recovered correctly from the present MRT model. Applying the Taylor expansion to Eq. (39), and noting that Eq. (27), we can obtain the following equations at different orders of ϵ :

$$O(\epsilon^0): g_i^{(0)} = g_i^{(eq)}, \quad (41)$$

$$\begin{aligned} O(\epsilon^1): & \rho c_v \partial_{t_1} g_i^{(0)} + d_{1i} g_i^{(0)} \\ & = -\frac{1}{\Delta t} (\hat{\mathbf{M}}^{-1} \Lambda \hat{\mathbf{M}})_{ij} g_j^{(1)} + \hat{w}_i Q^{(1)}, \end{aligned} \quad (42)$$

$$\begin{aligned} O(\epsilon^2): & \rho c_v D_{1i} g_i^{(1)} + \rho c_v \partial_{t_2} g_i^{(0)} + \rho c_v \frac{\Delta t}{2} D_{1i}^2 g_i^{(0)} \\ & + (1 - \rho c_v) d_{1i} g_i^{(1)} + (1 - \rho c_v) \frac{\Delta t}{2} d_{1i}^2 g_i^{(0)} \\ & = -\frac{1}{\Delta t} (\hat{\mathbf{M}}^{-1} \Lambda \hat{\mathbf{M}})_{ij} g_j^{(2)} + \hat{w}_i \rho c_v \frac{\Delta t}{2} (\partial_{t_1})^2 T. \end{aligned} \quad (43)$$

Multiplying $\hat{\mathbf{M}}$ on both sides of the above equations, we can obtain the following equations in the moment space:

$$O(\epsilon^0): \quad \hat{\mathbf{m}}^{(0)} = \hat{\mathbf{m}}^{(eq)}, \quad (44)$$

$$O(\epsilon^1): \quad \rho c_v \mathbf{I} \partial_{t_1} \hat{\mathbf{m}}^{(0)} + \mathbf{d}_1 \hat{\mathbf{m}}^{(0)} = -\frac{1}{\Delta t} \Lambda \hat{\mathbf{m}}^{(1)} + \hat{\mathbf{M}} \hat{\mathbf{G}}^{(1)}, \quad (45)$$

$$\begin{aligned} O(\epsilon^2): \quad & \rho c_v \mathbf{I} \partial_{t_1} \hat{\mathbf{m}}^{(1)} + \mathbf{d}_1 \hat{\mathbf{m}}^{(1)} + \rho c_v \mathbf{I} \partial_{t_2} \hat{\mathbf{m}}^{(0)} \\ & + \rho c_v \mathbf{I} \frac{\Delta t}{2} \partial_{t_1}^2 \hat{\mathbf{m}}^{(0)} + \rho c_v \frac{\Delta t}{2} (2\partial_{t_1} \mathbf{d}_1) \hat{\mathbf{m}}^{(0)} \\ & + \frac{\Delta t}{2} \mathbf{d}_1^2 \hat{\mathbf{m}}^{(0)} \\ & = -\frac{1}{\Delta t} \Lambda \hat{\mathbf{m}}^{(2)} + \hat{\mathbf{M}} \hat{\mathbf{S}}^{(2)}, \end{aligned} \quad (46)$$

where $\mathbf{d}_1 = \hat{\mathbf{M}} \text{diag}[\mathbf{c}_0 \cdot \nabla, \dots, \mathbf{c}_4 \cdot \nabla] \hat{\mathbf{M}}^{-1}$, $\hat{\mathbf{G}}^{(1)} = [\hat{w}_0 Q^{(1)}, \dots, \hat{w}_4 Q^{(1)}]^T$, $\hat{\mathbf{S}}^{(2)} = [0.5 \hat{w}_0 \rho c_v \partial_{t_1}^2 T, \dots, 0.5 \hat{w}_4 \rho c_v \partial_{t_1}^2 T]^T$. In addition, $\hat{\mathbf{m}} = \hat{\mathbf{M}} \mathbf{g}$ is the moment function, and $\hat{\mathbf{m}}^{(eq)}$ is the equilibrium function in the moment space defined as

$$\hat{\mathbf{m}}^{(eq)} = \hat{\mathbf{M}} \mathbf{g}^{(eq)} = [T, 0, 0, \hat{w} T, 0]^T. \quad (47)$$

According to Eq. (45), we can rewrite the first-order equations in t_1 scale, but here we just present the first, second, and third ones since only these equations are useful in deducing the macroscopic equation,

$$\rho c_v \partial_{t_1} T = Q^{(1)}, \quad (48)$$

$$c_s^2 \partial_{x_1} T = -\frac{1}{\Delta t} \zeta_1 m_1^{(1)}, \quad (49)$$

$$c_s^2 \partial_{y_1} T = -\frac{1}{\Delta t} \zeta_2 m_2^{(1)}. \quad (50)$$

Note that $\mathbf{d}_1^2 \hat{\mathbf{m}}^{(0)} = (\mathbf{E} \cdot \nabla_1)(\mathbf{E} \cdot \nabla_1) \hat{\mathbf{m}}^{(0)}$ where $\mathbf{E} = (\mathbf{E}_x, \mathbf{E}_y)$, and $\mathbf{E}_x = \hat{\mathbf{M}} \text{diag}[\mathbf{c}_{0x}, \dots, \mathbf{c}_{4x}] \hat{\mathbf{M}}^{-1}$, $\mathbf{E}_y = \hat{\mathbf{M}} \text{diag}[\mathbf{c}_{0y}, \dots, \mathbf{c}_{4y}] \hat{\mathbf{M}}^{-1}$, we can also obtain the following equation for conservative variable T at t_2 scale:

$$\begin{aligned} \rho c_v \partial_{t_2} T + \partial_{x_1} \left(\hat{m}^{(1)} + \frac{\Delta t}{2} \hat{c}_s^2 \partial_{x_1} T \right) + \partial_{y_1} \left(\hat{m}^{(2)} + \frac{\Delta t}{2} \hat{c}_s^2 \partial_{y_1} T \right) \\ = 0. \end{aligned} \quad (51)$$

Substituting Eqs. (49) and (50) into Eq. (51), we have

$$\begin{aligned} \rho c_v \partial_{t_2} T = \partial_{x_1} \left[\Delta t \left(\frac{1}{\zeta_1} - \frac{1}{2} \right) \hat{c}_s^2 \partial_{x_1} T \right] \\ + \partial_{y_1} \left[\Delta t \left(\frac{1}{\zeta_2} - \frac{1}{2} \right) \hat{c}_s^2 \partial_{y_1} T \right]. \end{aligned} \quad (52)$$

Based on Eq. (48) and Eq. (52), we can get

$$\rho c_v \partial_t T = \nabla \cdot (\lambda \nabla T) + Q, \quad (53)$$

where $\lambda = \Delta t (\zeta_1^{-1} - 0.5) \hat{c}_s^2 = \Delta t (\zeta_2^{-1} - 0.5) \hat{c}_s^2$.

The above procedure shows that the temperature equation can be recovered correctly from the present MRT model, and since the convection term is actually treated as a source term, the nondiagonal relaxation time used in [31] is not needed. In addition, the temperature gradient appeared in the source term Q can also be calculated locally in the present

MRT model, and Eqs. (49) and (50) give the corresponding algorithm.

C. Wetting boundary condition

To model fluid-solid interactions, the geometric formulation proposed by Ding and Spelt [51] is adopted in our following simulations, which can be expressed as

$$\rho_{x,0} = \rho_{x,2} + \tan \left(\frac{\pi}{2} - \theta^{eq} \right) |\rho_{x+1,1} - \rho_{x-1,1}|, \quad (54)$$

where θ^{eq} is an analytical prescribed equilibrium contact angle, and $\rho_{x,0}$ denotes the fluid density at the ghost layer next to the solid boundary. Here the first index in $\rho_{x,y}$ represents the coordinate along the horizontal solid wall, while the second one denotes the coordinate normal to the solid wall. In addition, the phase interface position is defined as $\rho = 0.5(\rho_l + \rho_g)$ throughout this work, in which ρ_l , ρ_g are the liquid density and gas density, respectively.

IV. RESULTS AND DISCUSSION

In this section several benchmark liquid-vapor phase change problems are selected to validate the performance of our proposed LB model. These typical examples include the D^2 law for droplet evaporation, droplet evaporation on heated surfaces, and bubble nucleation and departure in nucleate boiling. In addition, unless otherwise specified, the aforementioned MRT model is adopted in our simulations for its good numerical accuracy and stability. Moreover, it should be noted that apart from the relaxation times related to physical parameters, the other relaxation factors in the velocity field are the same as those used in the work of Li *et al.* [34], while they are all set to 1.0 for the temperature field.

A. Validation of the D^2 law

We first validate the present thermal LB model by considering the droplet evaporation in open space, and it is well known that the variation of the droplet diameter in this problem is described by the D^2 law, which states that the square of the evaporating droplet diameter D decreases linearly with time [52],

$$\left(\frac{D}{D_0} \right)^2 = 1 - \kappa t, \quad (55)$$

where D_0 is the droplet initial diameter and κ is the evaporation constant. The computational domain in our simulations is a square cavity, and the lattice size of it is set to be 200×200 . Initially, a droplet with a diameter of $D_0 = 60$ is located at the center of the cavity, and the temperature of the droplet is equal to the saturation temperature $T_{sat} = 0.86T_c$, while a higher temperature of $T_g = 1.0T_c$ is assigned to the surrounding vapor phase. In such a case, the droplet is expected to evaporate as a result of the temperature gradient around the liquid-vapor interface. In addition, the Dirichlet boundary (i.e., $T = T_g$) is adopted for the temperature field, which can be easily established by employing the halfway bounce-back scheme [53]. For the velocity field, the periodic scheme is used to determine the unknown density distribution functions streaming from the outside of the boundary [17]. The thermal

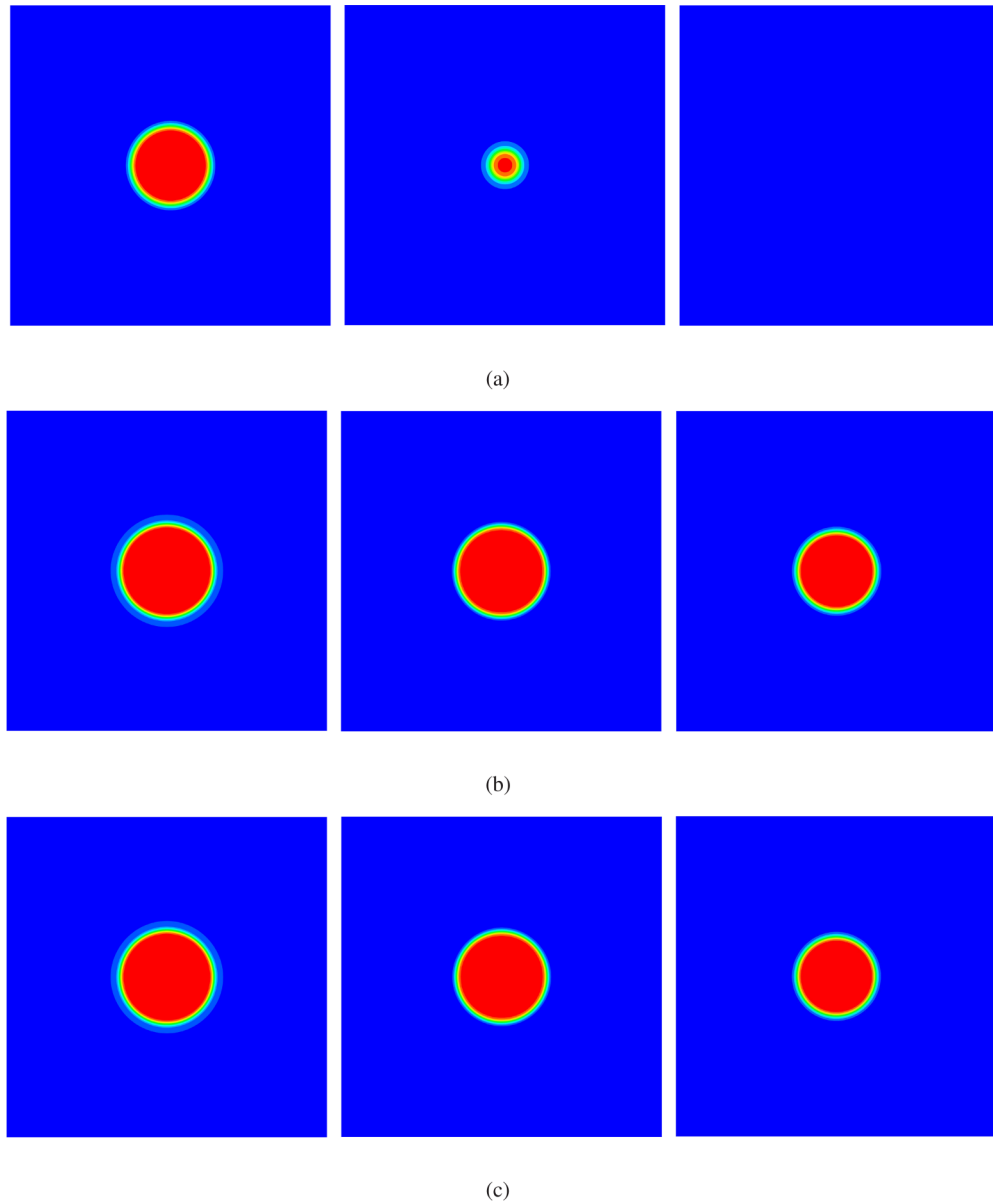


FIG. 1. Comparisons of the density contours given by the Gong-Cheng model (a), the proposed model (b), and the WENO scheme (c) at $t^* = 0.1$, $t^* = 0.25$, and $t^* = 0.75$ (from left to right).

conductivity, the kinematic viscosity, and the specific heat at constant volume are chosen as $1/3$, 5.0 , and 0.1 in the whole domain, which are all the same as previous works [28,31].

Figure 1 presents the density contours at different dimensionless time $t^* = t/t_{\text{total}}$. In order to test the numerical performance of the present LB model, the results obtained from the Gong-Cheng [27] model and the fifth-order finite difference weighted essentially nonoscillatory (WENO) scheme [54] are also included in this figure. It is clear that the simulation results using the present LBM agree well with the WENO scheme, which suggests that the present model could provide acceptable numerical results in simulating liquid-vapor phase change. However, it is noted that the evaporation rate predicted by the Gong-Cheng model [27] is much larger than the present LB and the WENO schemes, which is caused by the incorrect treatment of the temperature equation (see Sec. III A for details). To have a better understanding on this

statement, the time evolution of the square of the dimensionless diameter is also presented in Fig. 2, in which the results obtained with the work in [28] and [31] are also incorporated. As seen from this figure, apart from the the Gong-Cheng model [27], all of the other models follow the D^2 law. On the other hand, although the numerical results obtained from the present model and [31] agree well with the WENO scheme, the current model is more concise.

B. Droplet evaporation on a heated surface

Since the solid surface is usually encountered in most liquid-vapor phase transition problems, in the following we intend to study the problem of the droplet evaporation on a heated surface, which is a standard simple test for liquid-vapor phase change. Apart from the thermal diffusivity is taken as $\eta = 0.08$, the setup of the other physical parameters are the

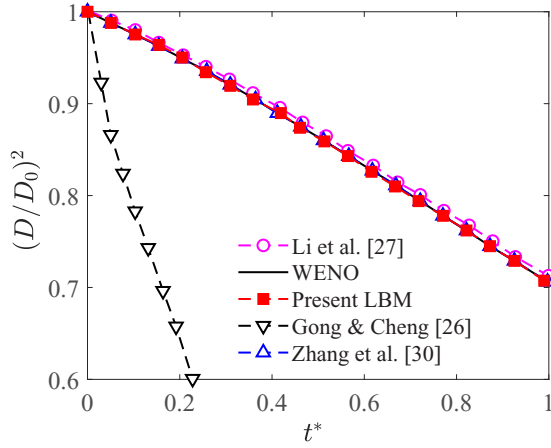


FIG. 2. Time evolution of the square of the dimensionless diameter for different models.

same as the first example. The physical domain is a rectangular enclosure which is covered by 100×200 mesh points. The bottom wall is a solid wall with a contact angle of 90° , and it is maintained at a temperature of T_h in the simulations, while the temperature for the top wall is taken as T_s . The open boundary condition and the periodic boundary condition are imposed at the top wall and the horizontal direction, respectively. Initially, the density and velocity are set according to

$$\rho = \frac{\rho_l + \rho_g}{2} - \frac{\rho_l - \rho_g}{2} \tanh\left(\frac{|\mathbf{x} - \mathbf{x}_0| - R_0}{0.5w_{lg}}\right), \quad (56)$$

$$\mathbf{u}(\mathbf{x}, 0) = \mathbf{0}, \quad (57)$$

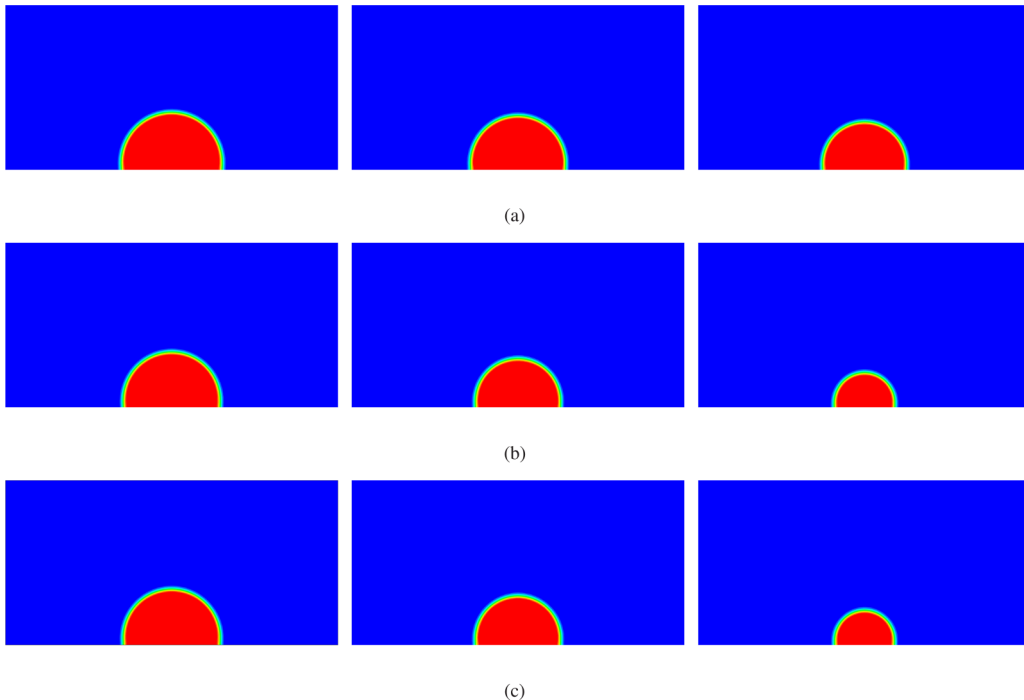


FIG. 3. Comparisons of the density contours given by the Gong-Cheng model (a), the proposed model (b), and the WENO scheme (c) at $t^* = 0.1$, $t^* = 0.25$, and $t^* = 0.75$ (from left to right).

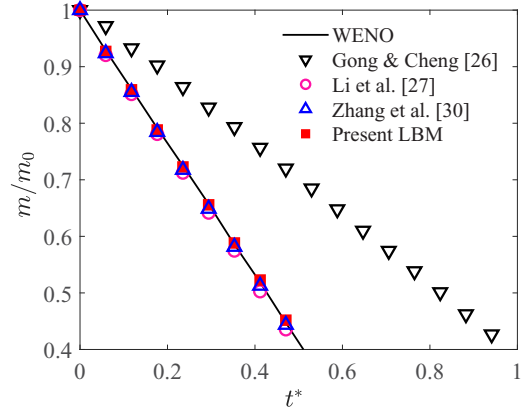


FIG. 4. Time evolution of the dimensionless droplet mass for different models.

where $\mathbf{x}_0 = (100\Delta x, 0)^T$, $R_0 = 35\Delta x$, and w_{lg} is chosen as $5\Delta x$. The simulation is first conducted without evaporation until the contact angle of the droplet equals the prescribed value.

The comparisons of density contours among the Gong-Cheng, present, and WENO solutions are shown in Fig. 3, where the density distributions from our model and WENO schemes match very very well, but the evaporation process predicted by the Gong-Cheng model [27] is a little bit slower than the other two models, and we note that a similar phenomenon is also reported by Li *et al.* [28] and Zhang *et al.* [31]. In order to further validate our model, the variations of the normalized droplet mass for different models are also depicted in Fig. 4. It is seen that apart from the Gong-Cheng model [27], the other solutions have excellent agreement.

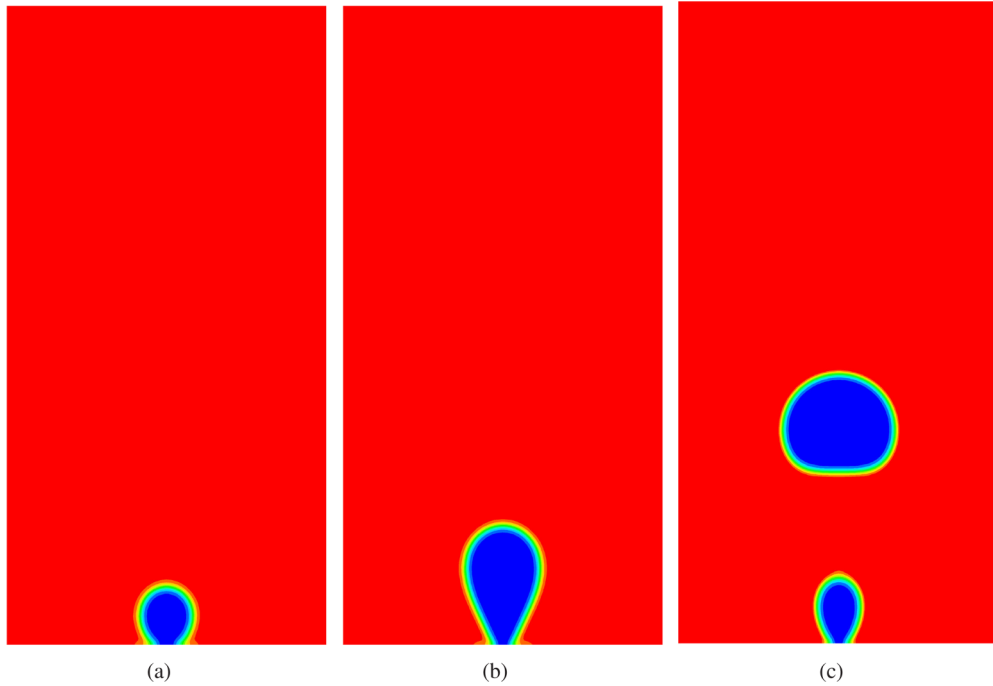


FIG. 5. Distributions of the density contours in nucleate boiling at $t = 5000\Delta t$ (a), $t = 10000\Delta t$ (b), and $t = 16000\Delta t$ (c) ($g = 3.0 \times 10^{-5}$).

C. Bubble nucleation and departure

Last, to show the potential of the present model, we consider a extremely complex liquid-vapor phase change problem of bubble nucleation and departure in nucleate boiling. In our simulation, the computational mesh is a 150×300 rectangular domain with the periodic boundary condition in the horizontal direction. Initially, the enclosure is filled with the saturated water, and the temperature within the domain is set to $T_{\text{sat}} = 0.86T_c$. For the velocity field, the bottom surface is the solid wall imposed by the no-slip boundary condition, while the open boundary condition [55] is used for the top plane. Apart from the central five grids at the bottom wall with a higher temperature of $T = 1.05T_c$, the temperatures at the rest of the bottom and top walls are all fixed at T_{sat} in the simulations.

The physical parameters used in the fluid field are the same as previous cases, while the thermal conductivity here is set to $2/3$, and the contact angle at the solid surface is equal to 75° . In addition, a buoyant force given by $\mathbf{F}_b = (\rho - \rho_{\text{ave}})\mathbf{g}$ is applied in the vertical direction, in which ρ_{ave} is the mean density over the whole domain, and $\mathbf{g} = (0, -g)$ is the gravity acceleration.

Figure 5 presents several typical snapshots of the nucleate boiling processes. It can be seen from Fig. 5 that owing to the influence of the high temperature, a small bubble is initially formed at the center of the solid wall. Then the size of the bubble gradually increases until it departs from the bottom wall. After that, the detached bubble moves upward under the effect of the buoyancy force, and a new bubble appears at the center of the solid wall, whose behavior is similar to the first bubble. To give a quantitative analysis, we follow the theoretical result given by Fritz [56], which states that the relationship between detachment bubble diameter and gravitational acceleration satisfying $D_d \propto g^{-0.5}$. To this end, simulations are carried out under different gravitational acceleration, and the corresponding results are shown in Fig. 6. It is clear that the detachment bubble diameter predicted by the present model is indeed proportional to $g^{-0.5}$, which further illustrates that our model is adequate for liquid-vapor phase change problems.

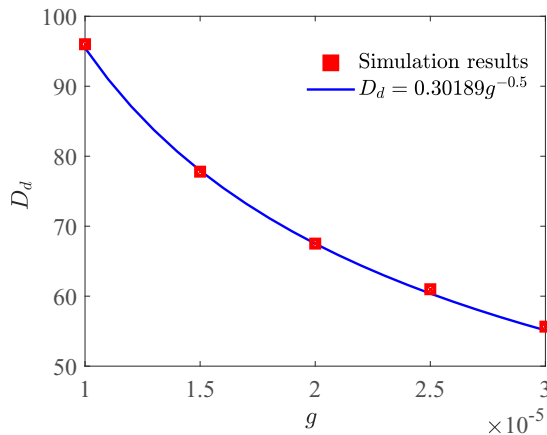


FIG. 6. Variation of detachment bubble diameter with gravity acceleration.

V. CONCLUSIONS

Liquid-vapor phase change phenomenon often arises in nature and scientific researchers, but numerical modeling of such problem still remains a challenging task in the LB community. The present work proposes a thermal lattice Boltzmann model for liquid-vapor phase change, which can correctly recover the temperature equation through multiscale analysis. In contrast

TABLE I. Comparisons of the stability and computational time per 10 000 steps between the present and previous models, in which $\hat{\zeta}$ denotes the relaxation times related to the “diffusion” coefficient (i.e., η or λ) and all the other free relaxation factors in Λ are set as 1.0; the symbols \checkmark and \times indicate that the corresponding method is stable and unstable, respectively.

	Present model		
	Li <i>et al.</i> [28]	Zhang <i>et al.</i> [31]	
Stability ($\hat{\zeta} = 1.0$)	\checkmark	\checkmark	\checkmark
Stability ($\hat{\zeta} = 2.0/3.0$)	\checkmark	\times	\checkmark
CPU time (s)	752.3894	1127.6723	984.2197

to previous models, the basic idea of the present model is that the temperature equation is treated as a pure diffusion equation with a source term. Additionally, in order to avoid the calculation of the gradient term of $\nabla(\rho c_v)$, a collision term is introduced to the evolution equation of the temperature distribution function, making it possible to retain the main merits of the LBM. Several numerical tests show that our approach could provide comparable results to the WENO scheme, and it is expected to be an efficient method in modeling liquid-vapor phase change.

ACKNOWLEDGMENTS

L.W. is grateful to Qing Li and Rongzong Huang for their useful discussions. We also would like to thank anonymous referees for their valuable comments which greatly improved the work. This work is financially supported by the National Natural Science Foundation of China (Grant No. 12002320).

APPENDIX A: ASSESSMENT OF THE PERFORMANCE OF THE PRESENT AND PREVIOUS MODELS

As mentioned previously, compared with some previous LB models for liquid-vapor phase change, the most striking feature of the present model is that it could avoid the calculations of some gradient terms [i.e., $\nabla(k\nabla T)$ and $\nabla(\rho c_v)$]. In this setting, the present method is expected to be more efficient than previous approaches. To better understand this point, in this Appendix, we intend to compare the numerical performance between the present and previous models. The problem considered is the droplet evaporation in open space, and the physical parameters used here are all the same as that adopted in Sec. IV A. Additionally, the custom C code is executed on a personal computer with Intel[®] Core[™] i7-9700 CPU at 3.0 GHz base frequency and 8.0 GB shared memory. The detailed comparison of the stability at different relaxation times $\hat{\zeta}$ and the computational time per 10 000 steps are

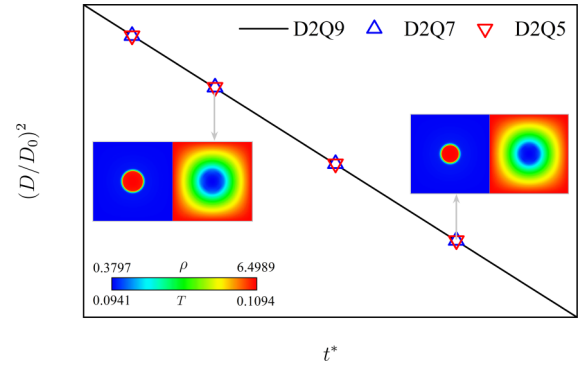


FIG. 7. Time evolutions of the square of the normalized diameter $(D/D_0)^2$ obtained from different lattices.

summarized in Table I. As shown in this table, due to the models developed by Li *et al.* [28] and Zhang *et al.* [31] are constructed using the D2Q9 lattice, the computational time of their models is much larger than our model, which suggests that the D2Q5 lattice used in our model is more efficient. In addition, it is noted that when the relaxation time $\hat{\tau}$ equals 2.0/3.0, it becomes unstable for the model of Li *et al.*, while the present model and that of Zhang *et al.* perform well. Because of these advantages, the present model could be a good candidate for simulating liquid-vapor phase change.

APPENDIX B: COMPARISON OF THE D2Q5, D2Q7, AND D2Q9 LATTICE MODELS

Because the temperature equilibrium distribution equation used in our model does not involve the second-order velocity term (also first-order term), it is possible to use the D2Q5, D2Q7, or D2Q9 lattice to simulate the liquid-vapor phase change in practical applications. In such a case, one may wonder if some differences exist when using these lattice models. To this end, this Appendix intends to conduct a comparison study for these lattice models. A series of numerical simulations for droplet evaporation in open space is performed again, and the time evolutions of the square of the normalized diameter $(D/D_0)^2$ obtained from different lattices are depicted in Fig. 7, in which the two snapshots of the local density and isotherms are also presented. From this figure, it can be seen that the D^2 law is well predicted by all lattice models, and the numerical difference among these models is so insignificant that it can be neglected. In addition, we note that the D2Q9 and D2Q7 lattice models require 952.0031 sec CPU time and 809.2025 sec CPU time, respectively, while the D2Q5 lattice needs only 752.3894 sec CPU time. Thus, from the point of view of computational efficiency, the D2Q5 lattice model is recommended.

- [1] R. Wen, X. Ma, Y. C. Lee, and R. G. Yang, Liquid-vapor phase-change heat transfer on functionalized nanowired surfaces and beyond, *Joule* **2**, 2307 (2018).
 [2] H. J. Cho, D. J. Preston, Y. Zhu, and E. N. Wang, Nanoengineered materials for liquid-vapor phase-change heat transfer, *Nat. Rev. Mater.* **2**, 16092 (2016).

- [3] B. Widom and J. S. Rowlinson, New model for the study of liquid-vapor phase transitions, *J. Chem. Phys.* **52**, 1670 (1970).
 [4] S. G. Liter and M. Kaviany, Pool-boiling CHF enhancement by modulated porous-layer coating: Theory and experiment, *Int. J. Heat Mass Transfer* **44**, 4287 (2001).

- [5] M. E. Steinke and S. G. Kandlikar, An experimental investigation of flow boiling characteristics of water in parallel microchannels, *J. Heat Transfer* **126**, 518 (2004).
- [6] R. A. Taylor and P. E. Phelan, Pool boiling of nanofluids: Comprehensive review of existing data and limited new data, *Int. J. Heat Mass Transfer* **52**, 5339 (2009).
- [7] M. Dadhich and O. S. Prajapati, A brief review on factors affecting flow and pool boiling, *Renewable Sustainable Energy Rev.* **112**, 607 (2019).
- [8] S. Kakaç and B. Bon, A review of two-phase flow dynamic instabilities in tube boiling systems, *Int. J. Heat Mass Transfer* **51**, 399 (2008).
- [9] J. Liu, C. M. Landis, and H. Gomez, Liquid–vapor phase transition: Thermomechanical theory, entropy stable numerical formulation, and boiling simulations, *Comput. Methods Appl. Mech. Eng.* **297**, 476 (2015).
- [10] D. Jamet, O. Lebaigue, and N. Coutris, The second gradient method for the direct numerical simulation of liquid–vapor flows with phase change, *J. Comput. Phys.* **169**, 624 (2001).
- [11] G. Son, A numerical method for bubble motion with phase change, *Numer. Heat Transfer B* **39**, 509 (2001).
- [12] C. K. Aidun and J. R. Clausen, Lattice-Boltzmann method for complex flows, *Annu. Rev. Fluid Mech.* **42**, 439 (2010).
- [13] H. Huang, M. C. Sukop, and X. Y. Lu, *Multiphase Lattice Boltzmann Methods: Theory and Application* (John Wiley & Sons, New York, 2015).
- [14] Q. Li, K. H. Luo, and Q. J. Kang, Lattice Boltzmann methods for multiphase flow and phase-change heat transfer, *Prog. Energy Combust. Sci.* **52**, 62 (2016).
- [15] R. Huang, H. Y. Wu, and N. A. Adams, Mesoscopic Lattice Boltzmann Modeling of the Liquid-Vapor Phase Transition, *Phys. Rev. Lett.* **126**, 244501 (2021).
- [16] J. Huang, L. Wang, and K. He, Three-dimensional study of double droplets impact on a wettability-patterned surface, *Comput. Fluids* **248**, 105669 (2022).
- [17] T. Krüger, H. Kusumaatmaja, A. Kuzmin, O. Shardt, G. Silva, and E. M. Viggen, *The Lattice Boltzmann Method: Principles and Practice* (Springer, Cham, 2017).
- [18] Z. Guo and C. Shu, *Lattice Boltzmann Method and Its Applications in Engineering* (World Scientific, Singapore, 2013).
- [19] K. H. Luo, L. L. Fei, and G. Wang, A unified lattice Boltzmann model and application to multiphase flows, *Philos. Trans. R. Soc. A* **379**, 20200397 (2021).
- [20] Z. Dong, W. Li, and Y. Song, Lattice Boltzmann simulation of growth and deformation for a rising vapor bubble through superheated liquid, *Numer. Heat Transfer A* **55**, 381 (2009).
- [21] C. Zhang, H. Zhang, X. Zhang, C. Yang, and P. Cheng, Evaporation of a sessile droplet on flat surfaces An axisymmetric lattice Boltzmann model with consideration of contact angle hysteresis, *Int. J. Heat. Mass Transfer* **178**, 121577 (2021).
- [22] M. Sugimoto, Y. Sawada, M. Kaneda, and K. Suga, Consistent evaporation formulation for the phase-field lattice Boltzmann method, *Phys. Rev. E* **103**, 053307 (2021).
- [23] T. Sun and W. Li, Three-dimensional numerical simulation of nucleate boiling bubble by lattice Boltzmann method, *Comput. Fluids* **88**, 400 (2013).
- [24] A. Fakhari, M. H. Rahimian, and M. Krafczyk, Extended lattice Boltzmann method for numerical simulation of thermal phase change in two-phase fluid flow, *Phys. Rev. E* **81**, 036707 (2010).
- [25] R. Zhang and H. Chen, Lattice Boltzmann method for simulations of liquid-vapor thermal flows, *Phys. Rev. E* **67**, 066711 (2003).
- [26] A. Márkus and G. Házi, Simulation of evaporation by an extension of the pseudopotential lattice Boltzmann method: A quantitative analysis, *Phys. Rev. E* **83**, 046705 (2011).
- [27] S. Gong and P. Cheng, A lattice Boltzmann method for simulation of liquid–vapor phase-change heat transfer, *Int. J. Heat Mass Transfer* **55**, 4923 (2012).
- [28] Q. Li, P. Zhou, and H. J. Yan, Improved thermal lattice Boltzmann model for simulation of liquid-vapor phase change, *Phys. Rev. E* **96**, 063303 (2017).
- [29] X. Shan and H. Chen, Lattice Boltzmann model for simulating flows with multiple phases and components, *Phys. Rev. E* **47**, 1815 (1993).
- [30] Q. Li, Q. J. Kang, M. M. Francois, Y. L. He, and K. H. Luo, Lattice Boltzmann modeling of boiling heat transfer: The boiling curve and the effects of wettability, *Int. J. Heat Mass Transfer* **85**, 787 (2015).
- [31] S. Zhang, J. Tang, H. Wu, and R. Z. Huang, Improved thermal multiple-relaxation-time lattice Boltzmann model for liquid-vapor phase change, *Phys. Rev. E* **103**, 043308 (2021).
- [32] Q. Li, Y. Yu, and K. H. Luo, Improved three-dimensional thermal multiphase lattice Boltzmann model for liquid-vapor phase change, *Phys. Rev. E* **105**, 025308 (2022).
- [33] P. Yuan and L. Schaefer, Equations of state in a lattice Boltzmann model, *Phys. Fluids* **18**, 042101 (2006).
- [34] Q. Li, K. H. Luo, and X. J. Li, Lattice Boltzmann modeling of multiphase flows at large density ratio with an improved pseudopotential model, *Phys. Rev. E* **87**, 053301 (2013).
- [35] A. L. Kupershtokh, D. A. Medvedev, and D. T. Karpov, On equations of state in a lattice Boltzmann method, *Comput. Math. Appl.* **58**, 965 (2009).
- [36] R. Huang and H. Wu, Third-order analysis of pseudopotential lattice Boltzmann model for multiphase flow, *J. Comput. Phys.* **327**, 121 (2016).
- [37] S. Y. Chen and G. D. Doolen, Lattice Boltzmann method for fluid flows, *Annu. Rev. Fluid Mech.* **30**, 329 (1998).
- [38] P. Lallemand and L.-S. Luo, Theory of the lattice Boltzmann method: Dispersion, dissipation, isotropy, Galilean invariance, and stability, *Phys. Rev. E* **61**, 6546 (2000).
- [39] X. Shan, Pressure tensor calculation in a class of nonideal gas lattice Boltzmann models, *Phys. Rev. E* **77**, 066702 (2008).
- [40] D. M. Anderson, G. B. McFadden, and A. A. Wheeler, Diffuse-interface methods in fluid mechanics, *Annu. Rev. Fluid Mech.* **30**, 139 (1998).
- [41] R. B. Bird, W. E. Stewart, and E. N. Lightfoot, *Transport Phenomena*, 2nd ed. (John Wiley & Sons, New York, 2001).
- [42] Z. H. Chai and B. C. Shi, Multiple-relaxation-time lattice Boltzmann method for the Navier-Stokes and nonlinear convection-diffusion equations: Modeling, analysis, and elements, *Phys. Rev. E* **102**, 023306 (2020).
- [43] B. Shi and Z. Guo, Lattice Boltzmann model for nonlinear convection-diffusion equations, *Phys. Rev. E* **79**, 016701 (2009).

- [44] L. Wang, B. C. Shi, and Z. H. Chai, Regularized lattice Boltzmann model for a class of convection-diffusion equations, *Phys. Rev. E* **92**, 043311 (2015).
- [45] H. Yoshida and M. Nagaoka, Multiple-relaxation-time lattice Boltzmann model for the convection and anisotropic diffusion equation, *J. Comput. Phys.* **229**, 7774 (2010).
- [46] R. Z. Huang and H. Y. Wu, Lattice Boltzmann model for the correct convection-diffusion equation with divergence-free velocity field, *Phys. Rev. E* **91**, 033302 (2015).
- [47] A. Cartalade, A. Younsi, and M. Plapp, Lattice Boltzmann simulations of 3D crystal growth: Numerical schemes for a phase-field model with anti-trapping current, *Comput. Math. Appl.* **71**, 1784 (2016).
- [48] Y. L. He, Q. Liu, Q. Li, and W. Q. Tao, Lattice Boltzmann methods for single-phase and solid-liquid phase-change heat transfer in porous media: A review, *Int. J. Heat Mass Transfer* **129**, 160 (2019).
- [49] Q. Liu, Y. L. He, D. Li, and Q. Li, Non-orthogonal multiple-relaxation-time lattice Boltzmann method for incompressible thermal flows, *Int. J. Heat Mass Transfer* **102**, 1334 (2016).
- [50] D. Lycett-Brown and K. H. Luo, Multiphase cascaded lattice Boltzmann method, *Comput. Math. Appl.* **67**, 350 (2014).
- [51] H. Ding and P. D. M. Spelt, Wetting condition in diffuse interface simulations of contact line motion, *Phys. Rev. E* **75**, 046708 (2007).
- [52] S. Zheng, F. Eimann, T. Fieback, G. Xie, and U. Gross, Numerical investigation of convective dropwise condensation flow by a hybrid thermal lattice Boltzmann method, *Appl. Therm. Eng.* **145**, 590 (2018).
- [53] T. Zhang, B. C. Shi, Z. L. Guo *et al.*, General bounce-back scheme for concentration boundary condition in the lattice-Boltzmann method, *Phys. Rev. E* **85**, 016701 (2012).
- [54] G. S. Jiang and C. W. Shu, Efficient implementation of weighted ENO schemes, *J. Comput. Phys.* **126**, 202 (1996).
- [55] Q. Lou, Z. Guo, and B. Shi, Evaluation of outflow boundary conditions for two-phase lattice Boltzmann equation, *Phys. Rev. E* **87**, 063301 (2013).
- [56] W. Fritz, Berechnung des Maximalvolumens von Dampfblasen, *Phys. Z.* **36**, 379 (1935).